Analyst

ROYAL SOCIETY OF CHEMISTRY

PAPER

View Article Online
View Journal | View Issue

Check for updates

Cite this: *Analyst*, 2025, **150**, 4389

Electrochemical and plasmonic detection methods yield comparable analytical performance for DNA hybridization

Nicolas Fontaine, Arielle Dauphin, Miriam Gaida, Rosalie Simard and Philippe Dauphin-Ducharme *

DNA-based biosensors have been engineered for the measurement of different molecular targets. Depending on the means through which binding is transduced, this may introduce differences in analytical performance, especially when looking at the target's molecular weight and length. To address this question, we developed a combined approach of two commonly used transduction methods in DNA-based biosensors – electrochemistry and surface plasmon resonance – for concomitant surface interrogation. Specifically, we looked at the limits of detection and maximal responses of redox-reporter-modified DNA interfaces of increasing lengths binding to their complementary sequences. In doing so, along with comparable limits of detection, we observed that both methods produced similar sigmoidal target-responses that monotonically varied as a function of sequence length. We envision that our combined electrochemical-surface plasmon resonance (eSPR) approach showcases that SPR could be used as a first method to help engineer recognition elements before purchasing costly redox modifications, and in turn accelerate their translation into sensing platforms.

Received 15th July 2025,
Accepted 6th August 2025

DOI: 10.1039/d5an00741k

rsc.li/analyst

Open Access Article. Published on 06 August 2025. Downloaded on 5/29/2026 10:34:21 PM.
This article is licensed under a Creative Commons Attribution-NonCommercial 3.0 Unported Licence.

1. Introduction

DNA-based biosensors are versatile recognition elements for the measurement of various molecular targets, ranging from small molecules to large proteins and viruses.[1–4] Target binding is expected to affect the interfacial properties, which can be measured using various transduction means (optical,[5,6] electrochemical,[7,8] acoustic,[9,10] *etc.*[11]). Among the commonly used methods, electrochemistry and surface plasmon resonance (SPR) remain widely prevalent. This is because they support sensitive, rapid, and multiple measurements that can be adapted to a variety of chemistries. In electrochemistry, transduction is typically achieved *via* covalent attachment of a redox reporter or by immersion in a solution of a redox mediator, both of which result in monotonic changes in electron transfer properties based on target concentration.[8,12,13] In SPR, measurement of the local refractive index change induced by target binding allows for continuous and real-time monitoring of binding affinities and kinetics.[14–16] Thus, both electrochemistry and SPR provide quantitative insights into the interfacial properties of DNA-modified surfaces.

Given that signal transduction occurs differently between electrochemistry and SPR, one may hypothesize that their analytical performance may differ, notably when it comes to the target size. This is because the propagation of the surface plasmon decays over longer distances (~200 nm)[17,18] from the surface than at distances through which electron transfer occurs to support electrochemical signaling (<2 nm).[19,20] Consequently, one could assume that SPR provides a more sensitive approach than electrochemistry for larger molecules since the molar refractivity is proportional to the mass of the target as described by the Lorenz–Lorentz equation.[21] Electrochemistry, in contrast, could enable sensitive measurements of smaller targets as electron transfer occurs closer to the electrode surface.[20,22]

Curious about unraveling whether these hypotheses hold in DNA-based biosensors, we developed a combined electrochemical-surface plasmon resonance (eSPR) approach due to its concomitant ability to assess electrochemical and plasmonic signal transduction sensitivities. To date, eSPR has been used to discriminate between surface or DNA probe non-specific interactions.[23] It has also been used to enhance the analytical capabilities of SPR, notably for measurements in complex matrices *via* electrochemical modulation of the refractive index.[24,25] To our knowledge, there remains a lasting question whether there are differences in analytical performance (signal gain and limits of detection (LODs)) between

Département de chimie, Université de Sherbrooke, Sherbrooke, Québec J1K 2R1, Canada. E-mail: philippe.dauphin.ducharme@usherbrooke.ca

Open Access Article. Published on 06 August 2025. Downloaded on 5/29/2026 10:34:21 PM.
This article is licensed under a Creative Commons Attribution-NonCommercial 3.0 Unported Licence.

electrochemical and SPR transduction mechanisms for the same biomolecular target and surface. In response, we try to address this question by functionalizing gold prisms with DNA sequences of various lengths that are modified with a redox reporter to assess the influence of the target complement size and distance separating the reporter from the surface. We found that, in contrast to the above, both methods produced similar LODs and signal change dependencies as a function of target size for duplexes of >20 base pairs. Given these similarities in performance, we envision that SPR could be used as a label-free benchmark to rapidly screen different recognition elements without having to systematically resort to the costly redox reporter modification. We foresee that using SPR will thus accelerate the translation of recognition elements into electrochemical sensing platforms.

2. Results and discussion

We started by fabricating functionalized gold prisms. This briefly involves coating BK7 Dove prisms with a 50 nm Au layer that we cleaned in a plasma oven and *via* electrochemical means (Fig. S2).[26,27] As others have done in the past to fabricate electrochemical DNA-based biosensors,[28,29] we proceeded with a sequential functionalization protocol. This first consisted of modifying ~75% of the prism surface with methylene blue-modified DNA sequences solely composed of adenine and thymine bases (~75% thymines, Table S1) of varying lengths (between 5 and 60 nucleotides). We decided to rely on these unstructured sequences, as with their lengthening (and thus increasing mass), we expected to measure an increase in the plasmonic shift concomitant with a decrease in the electron transfer rate. We finally functionalized the entire prism with the alkanethiol 6-mercaptohexanol, leaving ~25% of the surface to act as a reference (only alkanethiol present).

Our modified prisms produced electrochemical and plasmonic responses. We interrogated those using an in-house eSPR system comprising a P4SPR from Affinité Instruments featuring polymeric fluidics enabling a four-channel sequential plasmonic reading (one reference channel along with three sensing channels for reproducibility purposes) and electrochemical interrogation (Fig. 1A). By inserting reference and

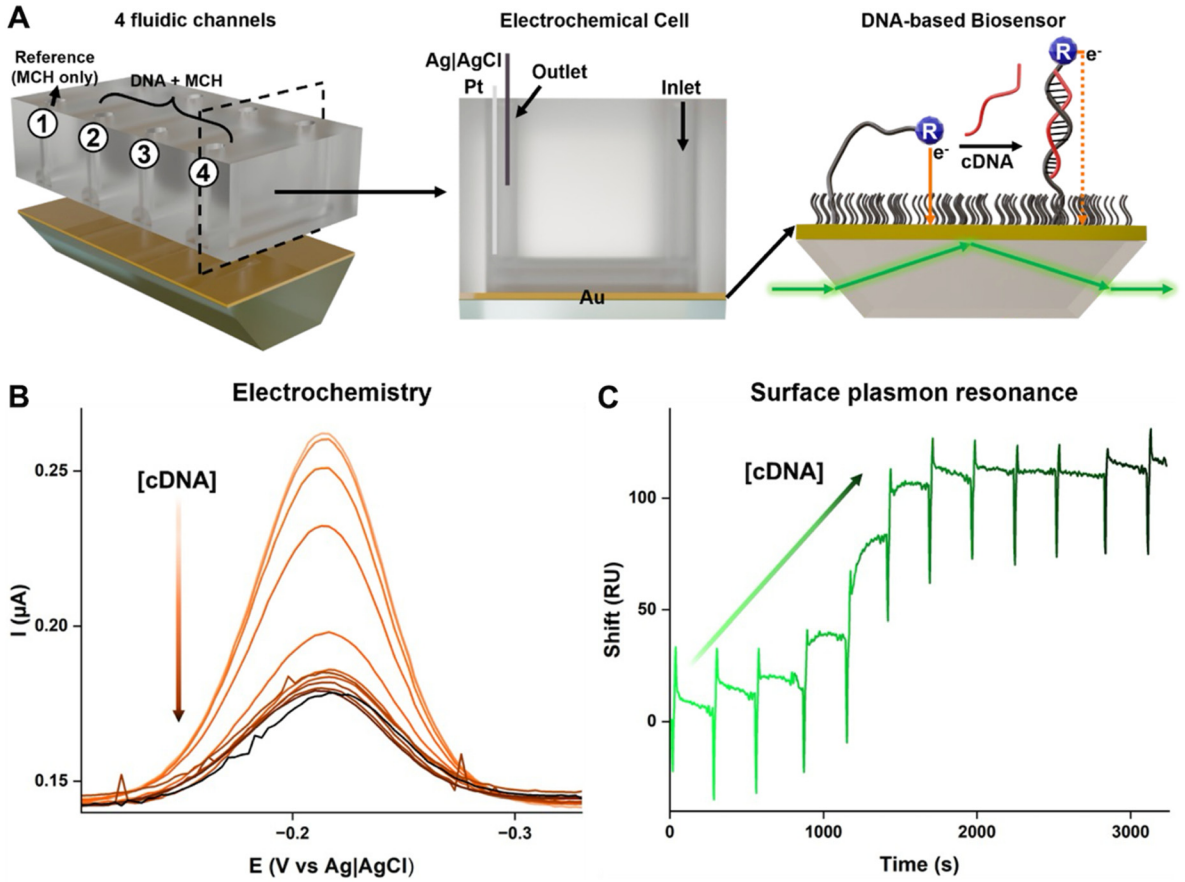

Fig. 1 (A) Our electrochemical-surface plasmon resonance surface is based on a gold film coated BK7 Dove prism mounted with a commercial polymeric fluidic chamber for the elution of samples. The electrochemical cell is formed by inserting platinum and Ag|AgCl electrodes in each outlet channel with the gold film functionalized with a redox reporter modified DNA sequence. (B) As a function of complement concentration, we monitor a peak current decrease (here in square-wave voltammetry with a frequency of 4 Hz) and (C) a positive plasmonic shift that we associate with target binding. Concentrations of complementary DNA (cDNA) are of 1×10^{-10}, 1×10^{-9}, 5×10^{-9}, 1×10^{-8}, 2.5×10^{-8}, 5×10^{-8}, 7.5×10^{-8}, 1×10^{-7}, 2.5×10^{-7}, 5×10^{-7}, 7.5×10^{-7} and 1×10^{-6} M.

This journal is © The Royal Society of Chemistry 2025

Open Access Article. Published on 06 August 2025. Downloaded on 5/29/2026 10:34:21 PM.
This article is licensed under a Creative Commons Attribution-NonCommercial 3.0 Unported Licence.

counter electrodes within each fluidic path, we obtained a three-electrode system for electrochemical interrogation through an electrical contact (copper tape) with the gold film for each channel. Electrochemical interrogation *via* cyclic voltammetry produced faradaic peaks with a reduction potential centered at ~−0.24 V *vs.* Ag|AgCl associated with the methylene blue redox reporter (Fig. S3B). As is commonly done,[27,30] integrating the methylene blue reduction peak returned surface coverages of 0.03–0.8 pmol cm^{-2}, exempt from chain–chain interactions[31,32] and which decreased with probe lengths (Fig. S3C), presumably due to steric constraints.[33]

The eSPR system reports on DNA hybridization. We verified this by circulating buffered solutions containing increasing amounts of the complementary DNA sequence while concomitantly measuring electrochemically (*via* square-wave voltammetry in Fig. 1B) and optically (Fig. 1C). As expected, we measured a decrease in the peak current and an increase in the refractive index. We hypothesize that the former is associated with a redox reporter having a slower electron transfer rate due to the more rigid duplex architecture,[34,35] while the latter is associated with a higher local refractive index arising from target binding in the vicinity of the plasmonic film.[36] When looking at the resulting eSPR binding traces, we found that both electrochemical and SPR responses followed hyperbolic binding,[25,37,38] which are correlated with target concentrations (Fig. 2A *vs.* Fig. 2B for a 60 nucleotide-long DNA duplex) with comparable dissociation constants (K_D values) of 13 ± 2 and 18 ± 3 nM reported as the mean and standard deviation of the three interrogation channels. Raw current and plasmonic signals, in contrast, varied vastly across the 3 sensing channels for both techniques (as opposed to the control channel, which remained unchanged (Fig. S5)), presumably due to variations in the amount of immobilized DNA. Normalizing the measured response with respect to the target-free signal counteracted this effect in electrochemistry, while reporting the reference-subtracted signal in SPR ensured a response arising from target binding (Fig. 2).

Limits of detection of DNA hybridization vary as a function of sequence length. When challenging prisms functionalized with DNA sequences of different lengths with increasing amounts of complement, we obtained electrochemical and plasmonic sigmoidal binding profiles (see Fig. S7 and S8 for all binding traces). The resulting LODs (see the SI for how this was determined) ranged from 4 to 96 nM with an overall decreasing trend as a function of increasing chain length using both methodologies (Fig. 3A). LODs are in agreement with past results for similar systems[38,39] as more bases provide a higher affinity. Only sequences containing 5 and 10 nucleotides did not provide a measurable change in the refractive index, which we presume to be due to: (1) the limited sensitivity of our eSPR system, (2) their lower melting temperatures (T_m, calculated to be ≤13 °C in comparison with >30 °C for longer sequences in solution (Fig. S6))[40] did not allow reaching saturation in the range of concentrations explored, resulting in a higher error, and (3) the decrease in the melting temperatures of DNA when tethered to a gold substrate.[41] We hypothesize that the electrochemical signal provided a response for these shorter sequences because of a possible interaction of methylene blue with DNA or that electrochemistry is more sensitive to smaller distance changes between the redox reporter and the surface.

Limits of detection are independent of the interrogation technique. Considering the increased distance (~3–40 nm) separating the redox reporter from the surface for the longer DNA complexes, which reduces the sensitivity of the electrochemical measurement (electron transfer occurs within 1–2 nm from the surface),[19,20] we observed no statistical difference in the electrochemical or plasmonic LODs (Fig. 3A). We hypothesize that this originates from: (1) a coincidental decrease in DNA surface coverage, a parameter that influences

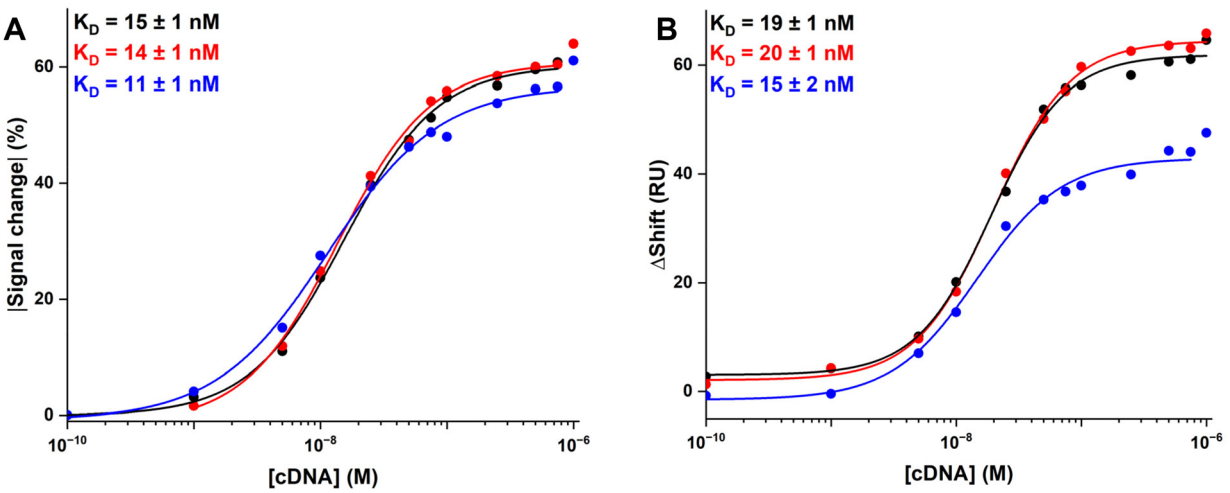

Fig. 2 We challenged our DNA-based sensors (here, a 60-nucleotide-long sequence) with their complementary sequence while concomitantly interrogating (A) electrochemically and (B) plasmonically. Doing so, we measured a decrease in peak current (shown here is the absolute signal change) and an increase in the plasmonic shift. The different colours correspond to independent measurements of the 3 sensing channels of the same prism.

Open Access Article. Published on 06 August 2025. Downloaded on 5/29/2026 10:34:21 PM.
This article is licensed under a Creative Commons Attribution-NonCommercial 3.0 Unported Licence.

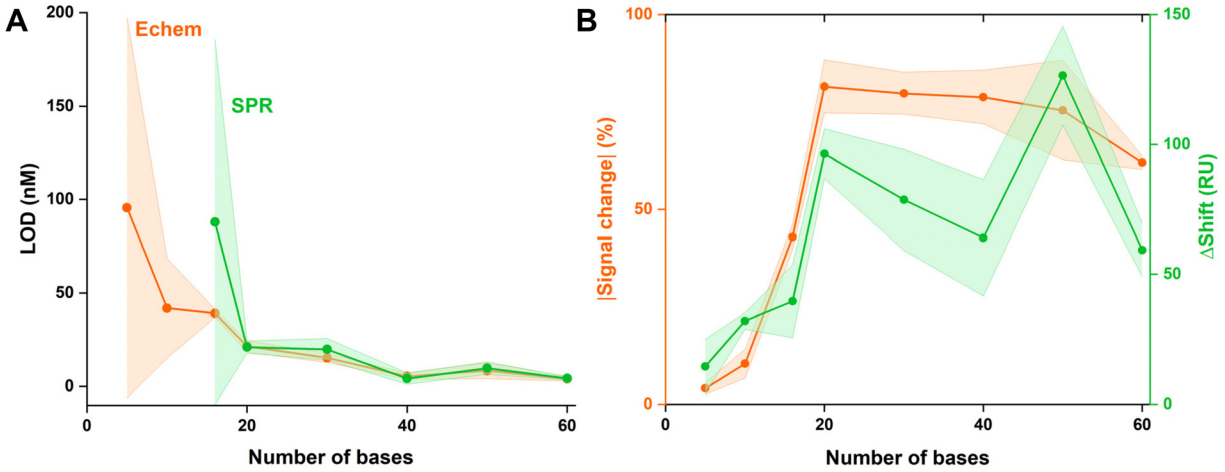

Fig. 3 We compared the electrochemical and plasmonic analytical performance using eSPR. (A) LODs decrease as a function of chain length and are comparable for sequences >16 nucleotides. (B) Looking at the magnitude of response (signal change for electrochemical measurements and ΔShift for plasmonic transduction) measured at a saturating concentration (1 μM) of the complementary sequence, we found a similar trend for both techniques. Shading represents the standard deviation of the three channels per prism for each condition.

plasmonic responses[42–45] and follows a similar trend (see below for more on this and in Fig. S3C and S9); and/or (2) DNA remaining proximal to the surface ("laying down") or exhibiting a sufficient range of motion for the reporter to approach for electron transfer[35] at lower target concentrations. Given the concordance of the electrochemical and plasmonic responses, we presume, as was previously reported,[46] that the latter hypothesis is more likely. This is because, while the plasmon can theoretically propagate farther from the prism surface, we envision that the first sequences generating a response will be found within short distances of the surface and where the enhanced electric field on flat surfaces is at its maximum (over 90% intensity at distances < ~25 nm).[18] These findings indicate that, as one would anticipate, the largest contribution in plasmonic and electrochemical signaling occurs within similar distances.

DNA surface coverage affects the analytical performance of both interrogation techniques. We explored this by fabricating gold films with three different DNA deposition concentrations of the 30-nucleotide-long sequence. At a lower DNA surface coverage, we only measured a hyperbolic response for the electrochemical signal (Fig. S9). We presume that this is because of instrumental limitation and the plasmonic signal being more dependent on the amounts of surface attached DNA.[28,34,44,45] At higher DNA surface coverages, in contrast, electrochemical and plasmonic signals returned a response from which we were able to determine LODs and maximum responses. While we measured a lower LOD for the lowest surface coverage, presumably because of prism degradation, all others were not statistically different. This further indicates that in having a sufficiently high DNA surface coverage, both methodologies provided comparable analytical performance.

The DNA length influences the magnitude of response, with similar trends for electrochemical and plasmonic means of transduction. We observed this when looking at the saturating sensor response (1 μM for ≥16 bases) for every DNA length (Fig. 3B). While we measured a lower maximal response from the smaller DNA duplexes, likely originating from the lower T_ms, we obtained similar responses of ~75% in electrochemistry and ~75 RU in SPR for the longer duplexes.[41] We presume that these results can be explained again based on how the signal is transduced in both methodologies. In electrochemistry, when at saturating target concentrations, DNA lengths >16 nt place the reporter at >2 nm distances, minimizing electron transfer. At the frequency of interrogation we used (4 Hz), this decrease did not maximize the saturating response (absence of a measurable faradaic peak), hence showing a plateau at 75% of the absolute signal change. When relying on SPR, we presume that the trend we measure is again the result of the plasmon being sensitive to phenomena occurring in the vicinity of the gold film. While the target molecular weight increased, the surface coverage varied with chain length (see Fig. S3C, S4 and S9), which changed the magnitude of the SPR maximal response. Moreover, the potential occurrence of an unstructured tail "laying" closer to the surface and the probability of partial DNA hybridization that increased for sequences >40 nucleotides could result in a response variability for the longer sequences, which would thus compensate for the lower amount of recognition element on the surface. Although there are mechanistic differences in signal generation, these phenomena could account for the similarities of trends observed in our eSPR system.

Our results suggest that we did not reach the limit in terms of detectable target size. For electrochemical interrogation, as long as we can electrochemically resolve lower amounts of DNA (and thus number of redox reporter) due to the diminished surface coverages, we presume that similar responses will be measured to the longest sequences we explored here. While electrochemical assessment of DNA hybridization typically employs shorter sequences of ~17–40 nt,[47,48] we envision,

This journal is © The Royal Society of Chemistry 2025

Open Access Article. Published on 06 August 2025. Downloaded on 5/29/2026 10:34:21 PM.
This article is licensed under a Creative Commons Attribution-NonCommercial 3.0 Unported Licence.

by extrapolating our results of the measurable peak current with our interrogation parameters and setup, that we could interrogate DNA interfaces modified with sequences of 90–120 nucleotides. In SPR, we foresee that measurements of larger sequences could be achieved. For instance, while studies focusing on perfect complementary sequences are of 18–22 nucleotide-long sequences,[49–51] the use of shorter sequences has achieved binding of 300–1500-long complements.[49,52] As is the case with electrochemistry, we also expect perfectly matching complements to reach a sequence length limit (something that remains to be explored) due to the lower DNA surface coverage capable of binding with the complement and driving plasmonic signaling. Given the resemblances in sensitivity we observed, we expect that both methodologies have similar suitability to investigate the effects of mismatches on DNA duplexes. We, however, envision that differences in signal transduction scheme performance would start to emerge when deploying in undiluted complex matrices. This is because SPR, in contrast to electrochemistry, is more prone to interferences from surface fouling and bulk refractive index changes since the plasmon decays farther from the substrate.[53,54] Combining both methodologies through eSPR could help overcome this challenge.

3. Conclusion

In this study, we developed a combined electrochemical-surface plasmon resonance setup for the characterization of DNA-based interfaces. We tested the analytical performance of our approach with DNA hybridization experiments using unstructured strands of varying lengths. When challenging sensors with their complementary targets, we obtained binding curves with similar LODs and magnitudes of response at saturating concentrations for both techniques. We presume that these similarities are because most signaling occurs within short distances (<2 nm) from the surface in both techniques. With these results on the similar sensitivities between electrochemistry and plasmonic readouts, we envision that the latter could be used to design recognition elements without having to resort to the costly redox reporter modification and, in turn, accelerate the screening of DNA sequences for different sensing applications.

Author contributions

N. F.: methodology, experiments, analysis, and writing. A. D.: experiments, methodology, analysis, and reviewing. M. G.: experiments, methodology, and analysis. R. S.: experiments and methodology. P. D. D.: supervision, funding, conceptualization, and reviewing. All authors have given approval to the final version of the manuscript.

Conflicts of interest

The authors declare no competing financial interests.

Data availability

The data supporting this article have been included as part of the SI.

Supplementary information is available. The document includes DNA sequences used in this study, as well as detailed procedures for our eSPR setup, substrates preparation. It does also describes how surface coverage, optimal SWV frequency, and LOD have been determined. Figures showing the raw signals obtained for both interrogation methodologies, calculated melting temperatures, all the binding curves obtained and the effect of surface coverage are also presented. See DOI: https://doi.org/10.1039/d5an00741k.

Acknowledgements

The authors would like to acknowledge the Canadian Foundation for Innovation through the John R. Evans Leaders Fund, the Natural Sciences and Engineering Research Council of Canada for funding this project *via* the Discovery grant program, and the Ministry of Economy, Innovation and Energy (MEIE) through the Fonds d'accélération des collaborations en santé. N.F. would like to acknowledge financial support through the Fonds de recherche du Québec - Nature et Technologies (FRQNT) through a postdoctoral fellowship. The authors convey special thanks to Stéphane Morin for gold deposition by PVD and Kevin Chabot for oxygen plasma cleaning, and advice on surface preparation. They would also like to thank Coline Beltrami, Paul G. Charette, Michael Canva, Khoa-Nam Nguyen, and Naïla Corcoran for insightful discussions.

References

1 Q. Wang, J. Wang, Y. Huang, Y. Du, Y. Zhang, Y. Cui and D. Kong, *Biosens. Bioelectron.*, 2022, **197**, 113739.
2 Y. Hua, J. Ma, D. Li and R. Wang, *Biosensors*, 2022, **12**, 183.
3 A. Kowalczyk, *Curr. Opin. Electrochem.*, 2020, **23**, 36–41.
4 M. Yu, T. He, Q. Wang and C. Cui, *Biosensors*, 2023, **13**, 889.
5 B. Kaur, S. Kumar, J. Nedoma, R. Martinek and C. Marques, *APL Photonics*, 2024, **9**, 091102.
6 L. Liang, F. Xie, L. Jin, B. Yang, L.-P. Sun and B.-O. Guan, *Adv. Sens. Res.*, 2025, **4**, 2400185.
7 G. A. Evtugyn, A. V. Porfireva and S. V. Belyakova, *J. Pharm. Biomed. Anal.*, 2022, **221**, 115058.
8 Y. Xiao, B. D. Piorek, K. W. Plaxco and A. J. Heeger, *J. Am. Chem. Soc.*, 2005, **127**, 17990–17991.
9 H. Dong, J. Huang, Z. Guo, P. Jia, Z. Sun, Y. Guo and X. Sun, *Microchem. J.*, 2024, **200**, 110344.
10 M. Pohanka, *Biosensors*, 2025, **15**, 197.
11 D. Lien, *Anal. Methods*, 2025, **17**, 1148–1159.
12 T. G. Drummond, M. G. Hill and J. K. Barton, *Nat. Biotechnol.*, 2003, **21**, 1192–1199.

Open Access Article. Published on 06 August 2025. Downloaded on 5/29/2026 10:34:21 PM.
This article is licensed under a Creative Commons Attribution-NonCommercial 3.0 Unported Licence.

13 S. S. Mahshid, S. Camiré, F. Ricci and A. Vallée-Bélisle, *J. Am. Chem. Soc.*, 2015, **137**, 15596–15599.
14 A. L. Chang, M. McKeague, J. C. Liang and C. D. Smolke, *Anal. Chem.*, 2014, **86**, 3273–3278.
15 S. Miura, S. Nishizawa, A. Suzuki, Y. Fujimoto, K. Ono, Q. Gao and N. Teramae, *Chem. – Eur. J.*, 2011, **17**, 14104–14110.
16 J. Zhou, Y. Wang and G.-J. Zhang, *Coord. Chem. Rev.*, 2024, **520**, 216149.
17 J. Homola, S. S. Yee and G. Gauglitz, *Sens. Actuators, B*, 1999, **54**, 3–15.
18 A. Abbas, M. J. Linman and Q. Cheng, *Biosens. Bioelectron.*, 2011, **26**, 1815–1824.
19 A. J. Bard, L. R. Faulkner and H. S. White, *Electrochemical Methods: Fundamentals and Applications*, John Wiley & Sons, 2022.
20 A. Barfidokht, S. Ciampi, E. Luais, N. Darwish and J. J. Gooding, *Anal. Chem.*, 2013, **85**, 1073–1080.
21 R. J. W. Le Fèvre, *Advances in Physical Organic Chemistry*, Elsevier, 1965, vol. 3, pp. 1–90.
22 H. Dong, X. Cao, C. M. Li and W. Hu, *Biosens. Bioelectron.*, 2008, **23**, 1055–1062.
23 S. E. Salamifar and R. Y. Lai, *Colloids Surf., B*, 2014, **122**, 835–839.
24 S. Patskovsky, A.-M. Dallaire and M. Meunier, *Sens. Actuators, B*, 2016, **222**, 71–77.
25 A.-M. Dallaire, S. Patskovsky, A. Vallée-Bélisle and M. Meunier, *Biosens. Bioelectron.*, 2015, **71**, 75–81.
26 O. R. Bolduc, L. S. Live and J.-F. Masson, *Talanta*, 2009, **77**, 1680–1687.
27 P. Dauphin-Ducharme, K. L. Ploense, N. Arroyo-Currás, T. E. Kippin and K. W. Plaxco, in *Biomedical Engineering Technologies: Volume 1*, ed. M. R. Ossandon, H. Baker and A. Rasooly, Springer US, New York, NY, 2022, pp. 479–492.
28 R. J. White, N. Phares, A. A. Lubin, Y. Xiao and K. W. Plaxco, *Langmuir*, 2008, **24**, 10513–10518.
29 T. M. Herne and M. J. Tarlov, *J. Am. Chem. Soc.*, 1997, **119**, 8916–8920.
30 J. M. Seibold, S. W. Abeykoon, A. E. Ross and R. J. White, *ACS Sens.*, 2023, **8**, 4504–4511.
31 Z. Zheng, S. H. Kim, A. Chovin, N. Clement and C. Demaille, *Chem. Sci.*, 2023, **14**, 3652–3660.
32 A. W. Peterson, R. J. Heaton and R. M. Georgiadis, *Nucleic Acids Res.*, 2001, **29**, 5163–5168.
33 F. Ricci, R. Y. Lai, A. J. Heeger, K. W. Plaxco and J. J. Sumner, *Langmuir*, 2007, **23**, 6827–6834.
34 P. Dauphin-Ducharme, N. Arroyo-Currás and K. W. Plaxco, *J. Am. Chem. Soc.*, 2019, **141**, 1304–1311.
35 Z. Zheng, S. H. Kim, A. Chovin, N. Clement and C. Demaille, *Chem. Sci.*, 2023, **14**, 3652–3660.
36 H. Šípová and J. Homola, *Anal. Chim. Acta*, 2013, **773**, 9–23.
37 F. C. Macazo, R. L. Karpel and R. J. White, *Langmuir*, 2015, **31**, 868–875.
38 Y. Gao, L. K. Wolf and R. M. Georgiadis, *Nucleic Acids Res.*, 2006, **34**, 3370–3377.
39 K. Bielec, K. Sozanski, M. Seynen, Z. Dziekan, P. R. ten Wolde and R. Holyst, *Phys. Chem. Chem. Phys.*, 2019, **21**, 10798–10807.
40 OligoAnalyzer Tool - Primer analysis and T_m Calculator | IDT, **https://www.idtdna.com/pages/tools/oligoanalyzer**, (accessed 19 March 2025).
41 H. Nasef, V. C. Ozalp, V. Beni and C. K. O'Sullivan, *Anal. Biochem.*, 2010, **406**, 34–40.
42 L. Simon, Z. Bognár and R. E. Gyurcsányi, *Electroanalysis*, 2020, **32**, 851–858.
43 C. E. Froehlich, J. He and C. L. Haynes, *Anal. Chem.*, 2023, **95**, 2639–2644.
44 L. Simon and R. E. Gyurcsányi, *Anal. Chim. Acta*, 2019, **1047**, 131–138.
45 T. Sakaki, K. Masuda, Z. Zhang, T. Yajima, H. Hasegawa, Y. Kim and O. Niwa, *Sens. Mater.*, 2022, **34**, 927.
46 E. A. Josephs and T. Ye, *ACS Nano*, 2013, **7**, 3653–3660.
47 N. Phares, R. J. White and K. W. Plaxco, *Anal. Chem.*, 2009, **81**, 1095–1100.
48 A. A. Lubin, B. Vander Stoep Hunt, R. J. White and K. W. Plaxco, *Anal. Chem.*, 2009, **81**, 2150–2158.
49 B. P. Nelson, T. E. Grimsrud, M. R. Liles, R. M. Goodman and R. M. Corn, *Anal. Chem.*, 2001, **73**, 1–7.
50 T. Schneider, N. Jahr, J. Jatschka, A. Csaki, O. Stranik and W. Fritzsche, *J. Nanopart. Res.*, 2013, **15**, 1531.
51 A. I. K. Lao, X. Su and K. M. M. Aung, *Biosens. Bioelectron.*, 2009, **24**, 1717–1722.
52 A. Kick, M. Bönsch, B. Katzschner, J. Voigt, A. Herr, W. Brabetz, M. Jung, F. Sonntag, U. Klotzbach, N. Danz, S. Howitz and M. Mertig, *Biosens. Bioelectron.*, 2010, **26**, 1543–1547.
53 J. Svirelis, J. Andersson, A. Stradner and A. Dahlin, *ACS Sens.*, 2022, **7**, 1175–1182.
54 K. M. Mayer and J. H. Hafner, *Chem. Rev.*, 2011, **111**, 3828–3857.

This journal is © The Royal Society of Chemistry 2025